PRELIMINARY INVESTIGATIONS OF LOW-NICKEL STAINLESS STEELS FOR STRUCTURAL APPLICATIONS

J. Kerr and R. Paton

Mintek, Private Bag X3015, Randburg. 2125. South Africa. E-mail: jonathank@mintek.co.za

ABSTRACT

The first stage of the development of a new modified 201-type low nickel austenitic stainless steel is described in this paper. The alloy is intended for use as a structural alloy, and so requires a yield strength >400MPa as well as acceptable weldability and toughness. The low nickel content will give a lower material cost in comparison to more conventional austenitic grades, and the processing route is required to be similar to that of Type 304 to keep the processing cost low. The base alloy was designed using empirical methods developed for stainless steel, and the properties of the base alloy were verified using a range of small-scale melts. The base alloy had a 0.2% proof strength of ~320-400MPa, and so it is planned to use V additions of ~0.15% to bring about precipitation strengthening in the hot rolled condition, so raising the alloy's proof strength above the 400MPa minimum.

1. INTRODUCTION

Over two thirds of all stainless steel manufactured falls within the AISI 300 series, and of these alloys, Type 304, 316 and their low carbon ("L") grades make up more than 80% of the volume sold. The most commonly made alloys, 304 and 304L, are metastable austenitic grades, and are considered general purpose stainless steels because of their good corrosion resistance, formability and weldability (304L). However, they are not commonly considered for use as structural materials except in situations where their corrosion resistance or toughness is an advantage.

The yield stress of Type 304 is typically ~250MPa, which is at the low end of strengths for C-Mn structural steels. By contrast, its cost is much higher. Nickel contributes 50% of the total operating costs in the manufacture of cold-rolled 304 [1], and so an obvious way to produce cheaper austenitic stainless steels is to replace the Ni with other austenite forming elements such as N, Mn and Cu. The 200-series of austenitic stainless steels uses a combination of Mn and N to replace part of the Ni. These types of alloys have a higher strength than Type 304; Type 201, which is the most commonly made of the 200-series, has a minimum proof stress of 330MPa. The higher strength is due to the higher nitrogen contents of these steels. Nitrogen is a strong interstitial solution strengthening element, adding ~65MPa to the yield strength for every 0.1% compared to 2MPa for 1% of Cr or Mn [2]. While this suggests that reducing the Ni content and increasing the N content of an austenitic grade should make it cheaper and stronger, the alloy design situation is more complex than this.

The benefit of C-Mn structural steels are that they give high strength per unit cost; the strengths can also be quite high (>400MPa) which allows more lightweight designs. The benefit of the conventional grades of austenitic stainless steels is that they possess a combination of good properties – corrosion resistance, toughness, weldability and formability. However their strength per unit cost is significantly higher than that of conventional structural steels. The design strategy for austenitic stainless steels suitable for structural applications must therefore focus on reducing the cost of the alloy while at the same time increasing its strength; corrosion resistance and formability are not as important, but the weldability should still be kept comparable to that of conventional austenitic alloys.

Such an alloy cannot replace the conventional structural steels, largely because its higher alloying contents will result in a steel that always has a higher material cost. It would find application in niches where its corrosion resistance or toughness would be of benefit in addition to its strength. Further reductions in cost and increases in strength would extend the range of applications for which it could be used.

The study reported in this paper is the initial phase in the development of a low Ni austenitic stainless steel for structural purposes. The purpose of this initial phase was to identify a base composition which would have the desired combination of strength and microstructure in the annealed state. Further work on this base alloy would entail the use of strengthening mechanisms other than solution strengthening and work hardening: i.e. precipitation hardening. A market study is being peformed in parallel with this work to identify potential niches for the alloy, but the results of this study will be reported at a later date.

2. ALLOY DESIGN

The criteria which were used to design an alloy with a higher strength-to-cost ratio than conventional austenitic stainless steels, were:

- The Ni content to be ≤2% and the Cr content to be <18% to reduce material costs to ~50% of that of Type 304.
- The alloy to have ~5% ferrite after solidification to ensure weldability.
- The alloy to have a yield strength ≥400MPa in the annealed or hot rolled condition.
- The alloy to be austenitic with good toughness and weldability.
- The alloy to have austenite stability similar to Type 304; i.e. no athermal martensite and limited strain induced martensite formation.
- The alloy to be amenable to standard manufacturing routes: hot rolling and annealing at conventional temperatures for Type 304.

Possible alloy compositions were screened using empirical and theoretical calculations for the critical properties in the design criteria. Since most of the calculation methods were developed for alloys quite different from the ones in the screening, the calculations were used more to identify problems or shortcomings with the alloys (e.g. strength far too low, insufficient austenite formation etc.), rather than to eliminate specific compositions. A composition range was identified in this way, and it is shown in Table 1.

Table 1. Composition of the new alloy.

Element	**New Alloy**		**201[3]**		**304[3]**	
	Low	**High**	**Low**	**High**	**Low**	**High**
C	0.02	0.08	0.04*	0.15	0.04*	0.08
Mn	8	10	5.5	7.5	1.2*	2
Si	0.3*	1	0.3*	1	0.3*	1
Cr	15	17	16	18	18	20
Ni	2	2	3.5	5.5	8	10.5
Cu	0.05	0.3	0.05*	0.2*	0.05*	0.2*
N	0.22	0.30	0.12*	0.25	0.01*	0.06*
Cr_{eq}	15.5	18.5	16.5	19.5	18.5	21.5
Ni_{eq}	7.3	10.5	7.8	15.4	9.0	14.3

* typical values which are not specified in the standard

Of prime importance in the design was to ensure an austenitic microstructure which would contain a small amount of ferrite after welding to prevent hot cracking. The Schaeffler diagram is commonly used to predict the microstructure of a stainless steel weld based on the balance of ferrite- and austenite-forming elements in the alloy. The diagram was used in this study in conjunction with Espy's equations[4] for the Cr and Ni equivalents (equations 1 and 2). The constitution range covered by the composition shown in Table 1 together with the typical ranges for Types 201 and 304 is shown in Figure 1. Although the new alloy does overlap part of the 201 constitutional range, its composition is different to 201. So properties not unduly different to those of Type 201 should be achievable in the new alloy but at lower Ni and Cr contents.

$$Cr_{eq} = \mathrm{Cr} + \mathrm{Mo} + 1.5 \times \mathrm{Si} + 0.5 \times \mathrm{Nb} + 5 \times \mathrm{V} + 2.2 \times \mathrm{Ti} + 3 \times \mathrm{Al} \tag{1}$$

$$Ni_{eq} = \mathrm{Ni} + 0.87 + 30 \times \mathrm{C} + \mathrm{Y} \times (\mathrm{N} - 0.045) + 0.33 \times \mathrm{Cu} \tag{2}$$

where Y = 30 for 0% < N < 0.2%
Y = 22 for 0.21% < N < 0.25%
Y = 20 for 0.26% < N < 0.35%

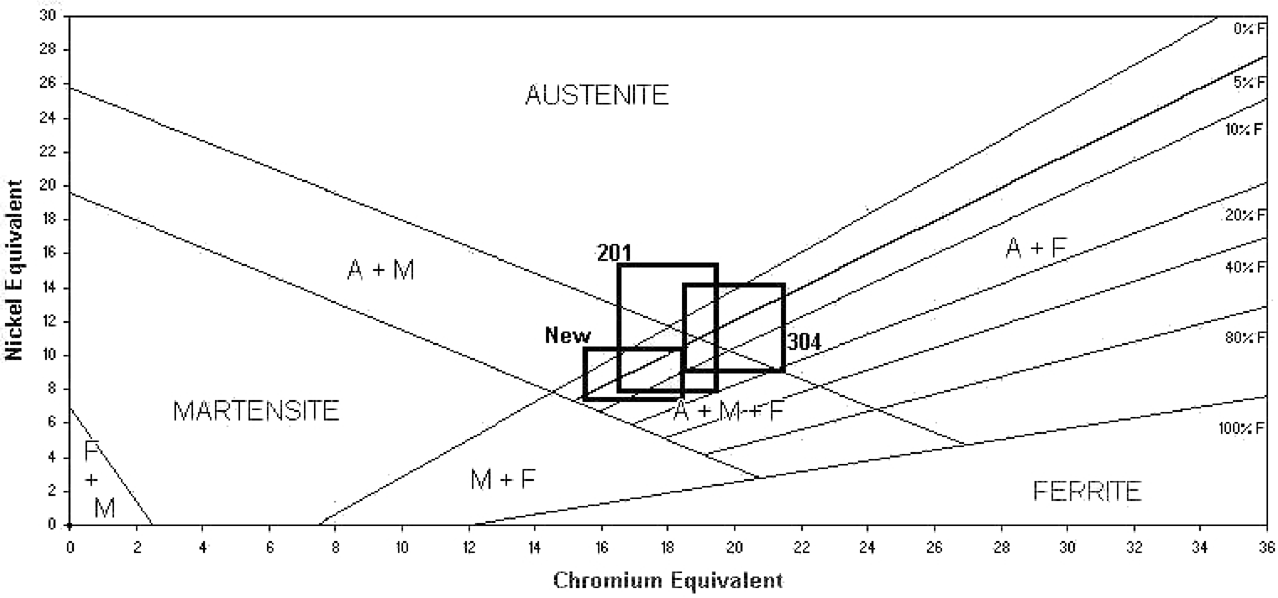

Figure 1. Schaeffler diagram showing the austenite-ferrite balance of the new alloy.

The stability of the austenite during deformation was modelled using Angel's correlation for the M_{d30} temperature[5], which is the temperature at which 30% deformation induces 50% transformation of austenite to martensite. Although the correlation was developed using Type 301 steels (16-18% Cr, 6-8% Ni, <0.15% C), the calculations can still be used to rank alloys: the lower the temperature, the more stable the austenite. Calculation of the M_{d30} for Type 304 compositions gives a range of 0 to 70°C; nevertheless, this alloy is sufficiently stable for cold rolling down to sheet. Angel's correlation is shown below:

$$M_{d30} = 413 - 13.7\mathrm{Cr} - 9.5\mathrm{Ni} - 8.1\mathrm{Mn} - 9.2\mathrm{Si} - 18.5\mathrm{Mo} - 462\mathrm{C} - 462\mathrm{N} \tag{3}$$

where M_{d30} = temperature at which 30% tensile deformation causes 50% transformation of austenite to martensite (°C)

Other properties such as the yield strength and nitrogen solubility were also modelled. As mentioned earlier, N exercises a large effect on the yield strength of austenitic stainless steels compared to other elements. A correlation, developed by Nordberg using results from austenitic and austenitic-ferritic stainless steels[2], predicted a strength for this alloy in the hot-rolled, austenitic condition (i.e. with a grain size of 60μm) of 343-386MPa. This strength is not considered high enough for structural use, and so it was deemed likely that another strengthening mechanism would be necessary. Nordberg's correlation is shown below:

$$R_{p0.2} = 120 + 210\sqrt{\mathrm{N} + 0.02} + 2\mathrm{Mn} + 2\mathrm{Cr} + 14\mathrm{Mo} + 10\mathrm{Cu} + (6.15 - 0.054\delta)\delta + (7 + 35(\mathrm{N} + 0.02))\mathrm{d}^{-0.5} \tag{4}$$

where $R_{p0.2}$ = 0.2% proof stress (MPa)
δ = ferrite content (volume %)
d = grain size (mm)

Nitrogen solubility in the liquid phase is reduced at higher temperatures. The solubility of N at 1600°C was calculated using standard activity calculations[6] and was found to be 0.21-0.24, which is lower than the N alloying range. However these alloys can be made in an induction furnace operating with an Ar atmosphere below atmospheric pressure. Arc welding could be problematic because of the high temperatures reached in the arc which will reduce the N solubility of the liquid weld metal. New Phacomp analysis[7] was used to estimate the solubility limit of N with respect to Cr_2N formation at 1050°C, and this was found to be 0.255-0.353. The same analysis showed that the formation of sigma phase was only likely below 900°C.

3. SMALL SCALE TESTING OF NEW ALLOY

The alloy modelling was validated by making a range of alloys which covered the design chemistry range, and performing simple tests on these alloys. The variations in the nominal compositions of the alloys are shown in Table 2. The levels of C, Mn, Cr and N, four elements critical to the austenite-ferrite phase balance and austenite stability with respect to martensite formation, were systematically varied. The microstructures were examined and the magnetic phase contents and hardnesses were measured. Eight alloys which fell within the composition of the new alloy were also subjected to tensile testing.

Table 2. Nominal composition variations in alloys used in screening tests.

C	**Alloy Numbers**	**Mn**	**Alloy Numbers**	**Cr**	**Alloy Numbers**	**N**	**Alloy Numbers**
0.02	1-12	6	1-6, 13-18	14	1-2, 7-8, 13-14, 19-20	0.2	Odd numbers
0.08	13-24	10	7-12, 19-24	16	3-4, 9-10, 15-16, 21-22	0.3	Even numbers
				18	5-6, 11-12, 17-18, 23-24		

These alloys were made in 50g melts which were prepared in a button arc furnace using a low pressure Ar atmosphere. The furnace had a water-cooled copper hearth, and so the cooling rate was high; although the arc temperature was always very high (>1800°C), the samples solidified within 30s. The combined ferrite and martensite content in the material as cast was measured magnetically using a Fischer Ferritescope. Samples were prepared for metallography and the balance of the material was annealed for 3.5h at 1050°C in order to homogenise and “austenitise” the samples. The Ferritescope was used to measure the magnetic phase content of the annealed samples and then they were prepared for metallography. Vicker’s hardness tests were also performed on the samples. The microstructures were checked for the presence of athermal martensite; when this phase was detected, a 40% KOH tint etch was used to reveal the presence of ferrite, and its volume fraction was measured using computerised image analysis.

The compositions of the alloys were measured by spark emission spectrometry; the nitrogen contents were not measured except for those samples which were later selected for mechanical testing. The compositions were used to predict the microstructures using Espy’s equations on the Schaeffler diagram. A comparison of the predicted to the measured ferrite contents using linear regression showed only a weak positive correlation. Figure 2 shows that the use of the analysis by Espy for these alloys in the as cast condition generally resulted in an under-prediction of the ferrite contents by an average factor of 2.2, whereas once the alloys had been austenitised at 1050°C for 3.5h, the factor dropped to 1.2 (Figure 3). When the annealing time at 1050°C was only 1.5h, which should have been sufficient for austenitisation, it was found that higher ferrite contents were measured. Thus it was likely that the small buttons used in this study had a significant degree of inhomogeneity, which resulted in higher ferrite contents being measured in the as cast condition. Larger melts should therefore agree more closely with Espy’s analysis and give a better correlation of predicted to measured ferrite contents.

Hardness measurements ranged from 180-220H_V for the austenitic and austenitic-ferritic alloys. There were no apparent relations between hardness and the composition. However, those alloys containing 14-16% Cr and 6% Mn did have higher hardnesses (240-400H_V), which were caused by the formation of athermal martensite during the rapid cooling after melting or water quenching after annealing.

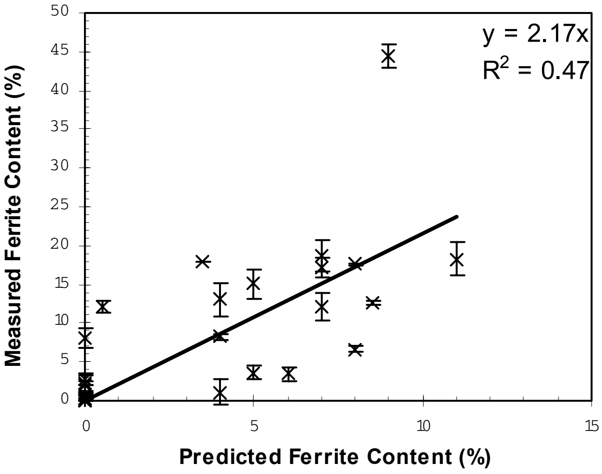

Figure 2. Comparison of ferrite content measured in the as cast condition to that predicted by Espy (error bars show 95% confidence intervals).

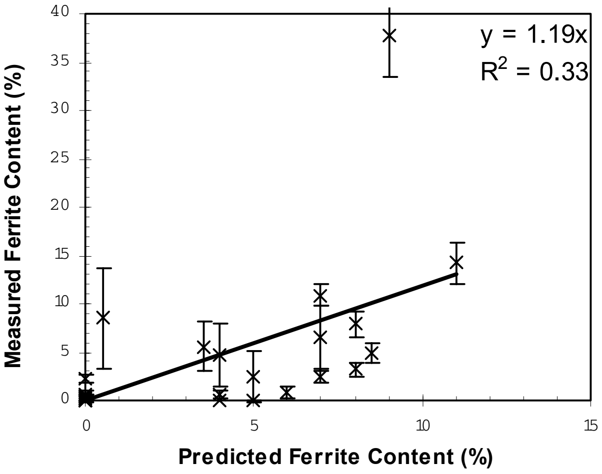

Figure 3. Comparison of ferrite content measured in the annealed condition to that predicted by Espy (error bars show 95% confidence intervals).

Eight alloys were selected for tensile testing; their compositions are shown in Table 3. The alloy buttons were annealed for 3.5h to homogenise and to austenitise them before they were cold rolled from ~8mm down to ~1mm. The materials work-hardened due to strain-induced martensite formation, and it was necessary to solution anneal the samples for 30 min after ~60% reduction (~3.2mm). Ferritescope readings were taken on the alloys after each annealing treatment, and also after cold rolling prior to the annealing treatments. The alloys were cut to give flat tensile specimens with a gauge of 25mm by 6mm. These specimens were annealed for 45min at 1050°C and then their hardnesses were measured using a Rockwell tester in order to check that the strain hardening had been completely removed. These specimens were tested at room temperature to ASTM specification E8. Ferritescope measurements were taken on the strained gauges near the failure site after testing to measure the amount of strain-induced martensite which had formed. Samples were also cut from the shoulders of the specimens and were used for grain size measurements on the longitudinal orientation. These measurements were made on metallographic samples using the ASTM comparative method[8].

Table 3. Compositions of alloys selected for tensile testing.

Alloy	**C**	**Si**	**Mn**	**Cr**	**Ni**	**Cu**	**N**	**Fe**
7-2	0.019	0.57	9.64	14.1	2.16	0.31	0.31	balance
8-2	0.017	0.50	10.6	14.4	2.07	0.37	0.29	balance
9-3	0.021	0.47	10.2	16.6	2.05	0.35	0.35	balance
10-2	0.019	0.50	10.8	14.9	2.02	0.35	0.15	balance
19	0.059	0.52	11.7	12.6	2.16	0.37	0.20	balance
20	0.049	0.54	10.6	14.3	2.09	0.35	0.19	balance
21-2	0.063	0.48	10.7	16.4	2.10	0.36	0.26	balance
22-2	0.091	0.58	8.23	16.4	2.13	0.38	0.22	balance

The proof stresses (Table 4) of the alloys ranged from 323MPa to 402MPa. Figure 4 shows how these results compared to those predicted using Nordberg's equation (equation 4). The alloy which showed the greatest deviation from the predicted proof stress was 9-3: its high N content implies that its strength should be substantially higher than that measured. It is possible that the nitrogen solubility limit was exceeded in this alloy, causing nitride precipitation: the predicted strength would have been lower in this case. However, no evidence of such precipitation was found.

Table 4. Tensile test results.

Alloy	0.2% Proof Stress		UTS		Elongation*	
	(MPa)	s	(MPa)	s	(%)	s
7-2	370	50.5	810	49.4	59	4.5
8-2	388	2.7	800	12.9	47	11.8
9-3	323	13.4	806	29.4	43	4.4
10-2	359	5.1	850	——	60	——
19	342	34.6	883	49.4	53	2.3
20	344	34.5	895	35.1	52	6.0
21-2	402	5.7	853	40.5	42	17.2
22-2	325	32.0	955	26.0	45	9.4

* Most samples broke outside the gauge length

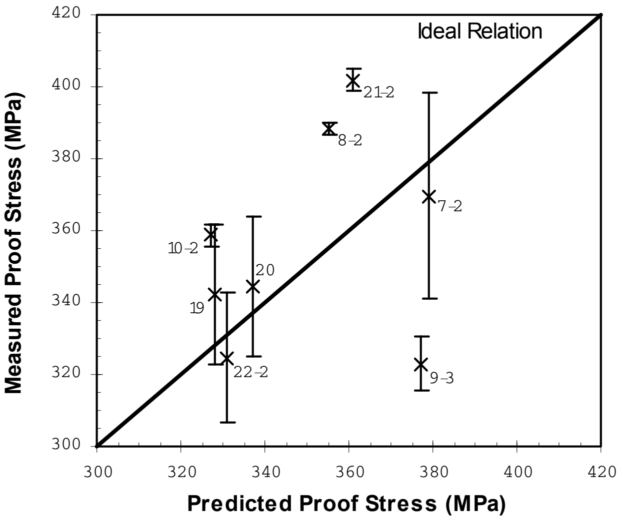

Figure 4. Comparison of measured proof stress to that predicted by Nordberg's equation[2] (error bars show the range of the measurements).

Measurements of the grain size and degree of martensite transformation which occurred in the specimen gauge are shown in Table 5 and it can be seen that the grain size was fairly coarse for cold rolled and annealed material (normally ASTM 6 to 8). Nordberg's equation (equation 4) includes the effect of grain size using a Hall-Petch relation (i.e. $R_{p0.2} \propto d^{-2}$). At the average N level of these alloys, an increase in grain size from 40μm to 60μm is predicted by the equation to be accompanied by a 15MPa reduction in the proof stress. So, had the alloys in Table 5 been hot rolled instead of cold rolled, their grain sizes would have been larger, and their proof stresses would have been lower by 15-30MPa.

Table 5. Longitudinal grain size and amount of martensite in the gauge of the tensile specimens.

Alloy	Grain size		Ferritescope Readings
	ASTM	(μm)	(%)
7-2	6	45	12
8-2	4 – 5	77.5	9
9-3	4 – 5	77.5	2
10-2	6 – 7	38.5	14
19	5	65	17
20	6	45	25
21-2	5 – 6	55	2
22-2	4 – 5	77.5	43

The ferritescope measurements on the gauges of the samples indicate the amount of strain-induced martensite which formed during the test. By comparison, Type 304 would be expected to form as much as 15-20% under similar conditions[9].

A number of factors influence the degree of strain-induced martensite formation, including grain size, the amount and type of deformation etc. Table 6 shows a comparison of the elongation, strain-induced martensite formation and the predicted M_{d30} temperature using Angel's correlation (equation 3). Also included are measurements of martensite formation during cold rolling (all the alloys were annealed prior to rolling). The trends in strain induced martensite formation were similar for both types of deformation. However, there was only a weak correspondence between the M_{d30} temperatures and martensite formation: alloys with higher M_{d30} temperatures generally had more martensite after deformation. Angel's correlation was developed using 301-type alloys, and so the N levels in the experimental alloys were substantially higher than the levels on which Angel based his analysis (0.010-0.053% for N). The results suggest that the austenite stabilisation effect of N may not be as great at these high levels as at the low levels in Angel's analysis (just as Espy proposed a reduced effect of N on austenite formation during solidification (equation 2)).

Table 6. Comparison of strain-induced martensite formation to M_{d30} temperatures.

Alloy	**Cold Rolling**		**Tensile Testing**		**M_{d30}**
	Martensite (%)	**Reduction (%)**	**Martensite (%)**	**Elongation (%)**	**(°C)**
304-2*	1	68	——	——	-61.7
7-2	24	66	12	59	-41.8
8-2	29	65	9	47	-42.7
9-3	14	66	2	43	-98.7
10-2	63	67	14	60	13.0
19	54	66	17	53	-6.2
20	42	66	25	52	-10.5
21-2	21	66	2	42	-78.6
22-2	46	67	43	45	-54.6

* tensile test results not reported

Alloy 22-2 showed a much higher degree of martensite transformation in comparison to the other experimental alloys. A possible reason for this was a combination of its low Mn level and the low strain rate used during the tensile testing (1mm/min ≈ 7×10^{-4}/s). Manganese is an effective austenite stabiliser, and slower strain rates allow more martensite formation[10]; so a combination of the two factors may have led to excessive austenite transformation. It is, however, unlikely that these two factors would have resulted in such a large increase in strain-induced martensite transformation as compared to the other alloys. Another possible reason for the lower degree of austenite stabilisation was that the N level was measured incorrectly and should have been lower than the 0.22% quoted. This would also have reduced the degree of austenite stabilisation. There is no evidence to support either of these hypotheses at present.

4. MATERIAL COST COMPARISON

The low Ni content of the new alloy gives it a lower material cost than either Types 201 or 304, as shown in Figure 5. The difference in materials cost relative to Type 304 only approaches the stated target of 50% when the Ni price is greater than $6/kg (as it has been for the past year or more). This cost difference can be maintained if the processing route is the same as that for 304. However, the alloy's strength offers no benefit over that of Type 201, and its hot rolled yield strength will be below the targeted 400MPa. It is intended to use V as a precipitation strengthening element to add an extra 100-150MPa to the hot rolled yield strength. The strengthening effect of precipitation hardening by VN formation in high Mn, low Ni austenitic stainless steels was estimated using data from reference [11]. The effect was ~95MPa for every 0.1% of V when the N content was in excess. ThermoCalc™ was used to model the effect of V on VN solution temperatures in the alloy. Figure 6 is a graphical representation of these results showing that there are two temperature regimes for VN stability. High temperature VN is necessary to ensure precipitation hardening will occur during hot rolling; therefore at least 0.15% V should be added to the steel. The estimated final strength of such an alloy would be ~500MPa. The effect of a V addition of 0.2% on the cost of the alloy is illustrated in Figure 5; although the addition is small, the cost of V units is similar to that of Ni units, and so the impact on cost is significant.

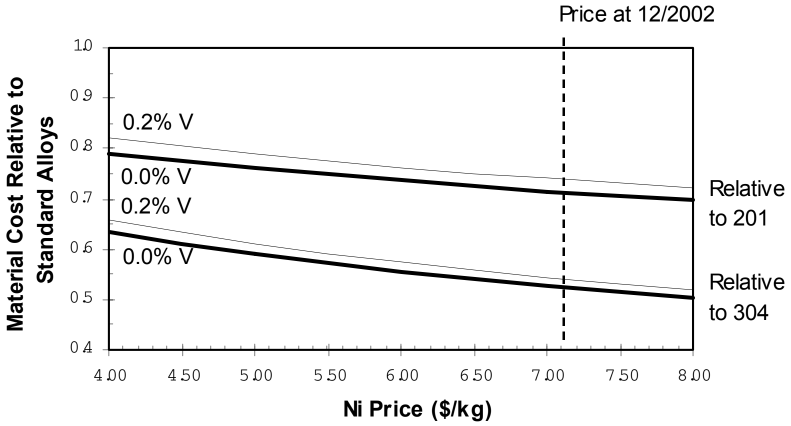

Figure 5. Material cost dependence on Ni price for the new alloy.

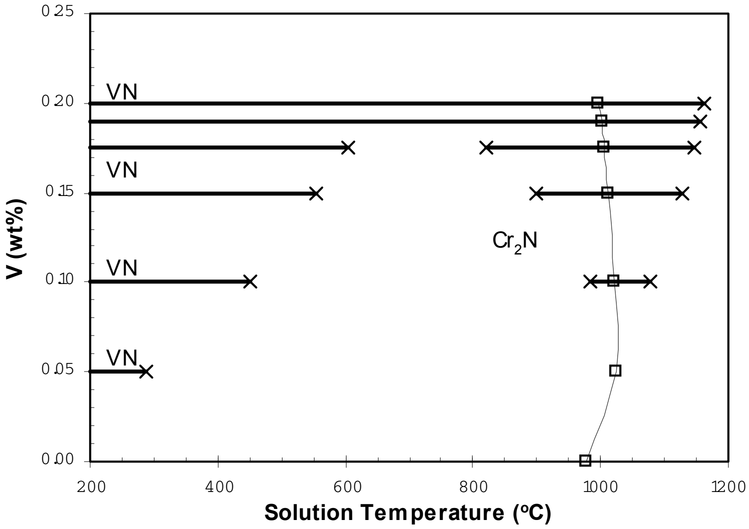

Figure 6. Calculated temperature stability ranges of VN precipitates in a 0.05% C, 0.5% Si, 8% Mn, 15% Cr, 2% Ni, 0.3% Cu, 0.25% N alloy.

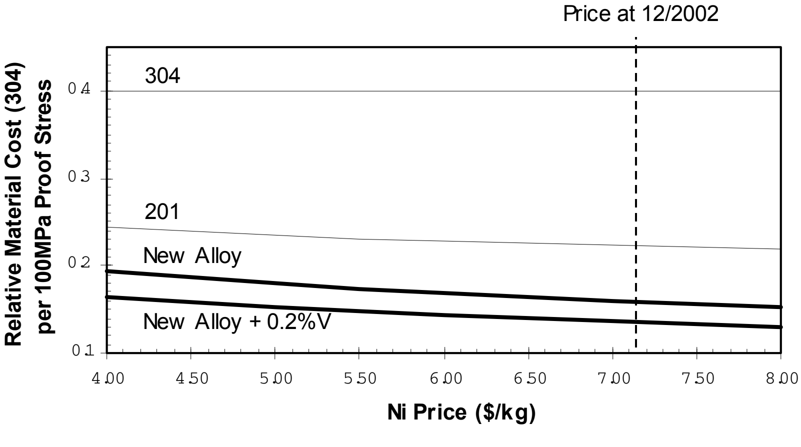

Figure 7. Cost relative to type-304 per 100MPa of minimum proof strength as a function of Ni price (minimum proof strengths: 250MPa for Type 304, 330MPa for Type 201 and the new alloy, 400MPa for the new alloy with 0.2% V).

Figure 7 shows the estimated material cost as a function of its minimum proof strength. In this figure, it can be seen that there is a cost benefit for the V addition if its strength is the primary criterion for its use. If the precipitation hardened alloy's selection is determined by its strength, it would give a minimum materials cost saving of 58% over Type 304 and 32% over Type 201.

5. CONCLUSIONS

A new austenitic stainless steel which is low in Ni and has a reduced Cr content with a high Mn and N content has been designed. The design process made use of a number of empirical and theoretical equations to model the effects of the composition on critical properties such as ferrite content and yield strength. The alloy is intended for use in structural applications and therefore requires a higher proof stress than can typically be obtained in austenitic alloys. The alloy described in this paper is considered the base alloy to which small additions of V will be added to increase the strength by precipitation hardening. It is hoped to report on this work in the future.

6. ACKNOWLEDGEMENTS

This paper is published by permission of Mintek. The authors wish to thank the South African Innovation Fund administered by the National Research Fund (NRF) for their sponsorship of this project.

7. REFERENCES

[1] Fritz, E., "Stainless steel production technology: trends, developments and new projects", Steel World, 2002, pp. 33-39.

[2] Nordberg, H., "Mechanical properties of austenitic and duplex stainless steels", Innovation Stainless Steel, Florence Italy, 1993, vol. 2, pp. 2.217 – 2.229.

[3] Davis, J. R. (ed.), Stainless Steels, ASM International, 1994.

[4] Espy, R. H., "Weldability of nitrogen-strengthened stainless steels", Welding Journal, 1982, vol. 61, pp. 149-156.

[5] Angel, T., "Formation of martensite in austenitic stainless steels", Journal of the Iron and Steel Institute, 1954, vol. 177, pp. 165-174.

[6] Balachandran, G., Bhatia, M. L., Ballal, N. B. and Rao, P. K., "Some theoretical aspects on designing nickel free high nitrogen austenitic stainless steels", ISIJ International, 2001, vol. 41 no. 9, pp. 1018-1027.

[7] Morinaga, M., Murata, Y. and Yukawa, H., "Recent progress in the New Phacomp approach", Minerals, Metals and Materials Society/AIME, Materials Design Approaches and Experiences, 2001 pp. 15-27.

[8] "ASTM E112-96: Standard Test Methods for Determining Average Grain Size", Annual Book of ASTM Standards 2002, vol. 03.01, pp. 251-274.

[9] Kanni Raj, A., Padmanabhan, K. A., "Formability of metastable austenitic stainless steel sheets: I Experimental" Transactions of the Indian Institute of Metals, 1998, vol. 51, pp. 201-215.

[10] Talyan, V., Wagoner, R. H., Lee, J. K., "Formability of stainless steel", Metallurgical and Materials Transactions A, vol. 29A, pp. 2161-2172.

[11] Whelan, G. W., Cordea, J. N., "Precipitate analysis in high nitrogen austenitic drill collar alloys", Conference Proceedings: High Manganese High Nitrogen Austenitic Steels, ASM International, 1992, pp. 67-76.